2017

Online prediction of battery discharge and flight mission assessment for electrical rotorcraft

Abdullah Alnaqeb
Iowa State University

Online prediction of battery discharge and flight mission assessment for electrical rotorcraft

by

Abdullah Alnaqeb

A thesis submitted to the graduate faculty

in partial fulfillment of the requirements for the degree of

MASTER OF SCIENCE

Major: Aerospace Engineering

Program of Study Committee:
Peng Wei, Major Professor
Chao Hu
Leifur Leifsson

The student author, whose presentation of the scholarship herein was approved by the program of study committee, is solely responsible for the content of this thesis. The Graduate College will ensure this thesis is globally accessible and will not permit alterations after a degree is conferred.

Iowa State University

Ames, Iowa

2017

DEDICATION

I only succeed by way of the Almighty

TABLE OF CONTENTS

Page

LIST OF TABLES

Page

LIST OF FIGURES

Page

ABBREVIATIONS

UAS ..... Unmanned Ariel Systems

eVTOL ..... electric Vertical Take-off and Landing

UTM ..... UAS Traffic Management

SOC ..... State of Charge

ECM ..... Equivalent Circuit Model

ODM ..... On-Demand Mobility

OCV ..... Open-circuit Voltage

DOC ..... Depth of Charge

PSO ..... Particle Swarm Optimization

NOMENCLATURE

Q	Capacity, Ah
V_m	Measured voltage, V
V_s	Simulated voltage, V
R_0	Resistance of resistor in series, ohm
R_1	Resistance of resistor in RC, ohm
τ	RC circuit time constant, sec
P	Power, W
T	Thrust, N
α	Angle of Attack, deg
γ	Flight path angle, deg
v_i	Induced velocity, m/s
m	mass of UAS, Kg
v_∞	Stream velocity, m/s
v_h	Hover velocity, m/s
η_P	Propeller efficiency
η_e	Power conversion efficiency
C_D	Drag coefficient
FA	Frontal area, m^2

ACKNOWLEDGMENT

First and foremost, I would like to express my sincere gratitude to my advisor Dr. Peng Wei for the continuous support of my master's study and research. His patience, motivation, enthusiasm, and immense knowledge were valuable throughout my time here at Iowa State. I could not have had a better advisor and mentor.

Additionally, I would like to thank the rest of my thesis committee; Dr. Chao Hu and Dr. Leifur Leifsson for their encouragement, insightful comments, and critical feedback.

My sincere thanks also goes to the System Realisability and Safety Lab led by Dr. Chao Hu and both of his students Yifei Li and Yu Hui Lui for offering all the help needed throughout this research work. Additionally I would like to personally thank Joshua Wallin and Priyank Pradeep for their support and guidance.

I thank my fellow labmates in the Intelligent Aerospace Systems Lab for all the fun we have had in the past 2 years. Also I would like to thank my personal friends Abdul Rahman Farraj, Ahmed Shareef, Hayder Mansoor, Mohammed El-amin and Mohammed Gizouli.

Last but not the least, I would like to thank my family, precisely my beloved parents, who without their continuous support, love, and prayers, I wouldn't be where I am today. They have allowed me to realize my own potential and for that I will be forever indebt. All the love they have provided me over the years was, and will always be, my life's greatest gift.

ABSTRACT

In recent concept development and research effort on Unmanned Arial System (UAS) Traffic Management (UTM) and urban on demand mobility (ODM), electric Vertical Take-off and Landing (eVTOL) operations for cargo delivery and passenger transportation need to constantly check if their mission can be successfully completed given the current battery power supply. This onboard or ground-based mission evaluation algorithm is necessary because (1) eVTOL aircraft run on limited battery power; and (2) eVTOL aircraft are usually light weighted so they are subject to wind uncertainties in low-altitude airspace. In this work, the plan is to create an equivalent circuit model (ECM) that best represents the battery pack of a UAS, and then use flight testing to validate the accuracy of that model. Additionally, the ECM will be used to predict the UAS's ability to complete a specific flight plan successfully. The expected significance of this research is to provide an online framework to constantly monitor and predict battery behavior for mission assessment, which is critical for low-altitude eVTOL operations.

CHAPTER 1. INTRODUCTION

1.1 Background

Electric Unmanned Arial Systems (UAS) have received significant attention in recent years. They are being deployed in a variety of areas like agriculture, cargo delivery, surveillance, and on-demand mobility (ODM). The FAA projects a rise in sales of UAS used for commercial purposes from 600,000 in 2016 to 2.7 million by 2020 [1]. This significant increase supports the necessity of developing a low-altitude UAS traffic management (UTM) system to help enable safe and efficient small UAS (sUAS) operations in this specific airspace. A UTM system should be designed to have certain major inputs, which include flight plans of the UAS aircraft, trajectories of the UASs, weather forecast, and airspace/terrain constraints, such as no-fly zones and airport restrictions [2].

NASA has initiated collaborative efforts with multiple government entities, industry, and academic institutions in order to pave the way for the development of UTM [2]. The main focus of the collaboration has been on sUAS operations, which include, but is not limited to, cargo delivery proposed by Amazon and Google [3, 4]. Since 2016, the possibility of urban ODM has been explored by NASA, Uber, Airbus and university researchers [3, 4, 5, 6, 7]. Most of UTM and ODM operations are based on Electric Vertical Take-Off and Landing (eVTOL) aircraft, where the battery runs on limited power and wind can have a huge effect in low altitude airspace due to the fact that they're mostly lightweight. In a huge number of eVTOL, the propuslion system is purely electrical. A few groups such as NASA Ames [8, 9] have worked on real-time estimation of battery state-of-charge and prediction of future power demand for fixed-wing aircraft.

1.2 Motivation

It is important to be able to assess a UAS's ability to successfully complete a mission given a specific flight plan. Figure 1.1 shows a use case where a package is being delivered from a warehouse

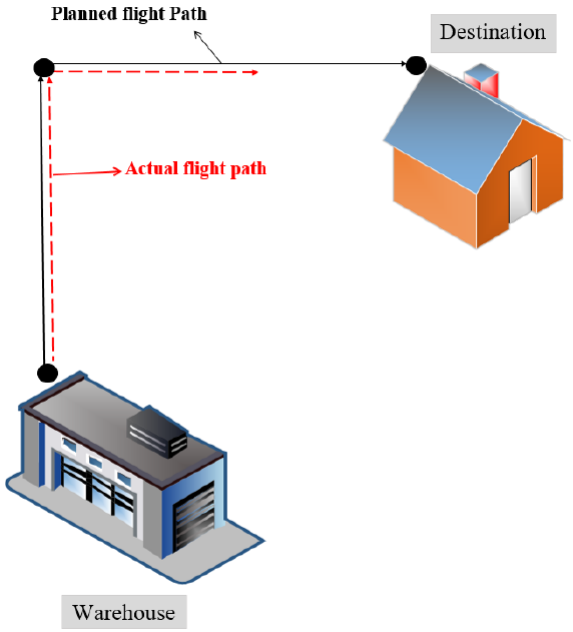

Figure 1.1: Use case

to a specified destination using the flight plan drawn. It is essential to ensure that the UAS has sufficient power in its battery to complete the mission. The inability to successfully complete the mission could have damages on the UAS as well as the surroundings, and that can be quite costly. The ability to predict whether or not a UAS has enough power left in the battery to complete a specific flight plan is critical in low altitude airspace.

1.3 Contributions

The main contribution of this work is the creation of an equivalent circuit model that best represents a cell of the UAS, and then extend that model to represent it on battery pack level.

Figure 1.2: DJI Phantom 3 Standard

Figure 1.3: DJI Phantom 3 Standard cell

As a proof of concept, the equivalent circuit model is then validated with the aid of flight testing data of the UAS. Lastly, an extra step is taken to use the equivalent circuit model to predict the UAS's ability to complete a specific flight mission.

1.4 Electric Vehicle Background

The vehicle used for the purpose of this work is the DJI Phantom 3 Standard, which has the largest market share [10]. With the aid of the DJI developer kit, current and voltage profiles of missions can be archived and save for analysis purposes [11]. This will prove to be vital for the state estimation algorithm described in section 4. The DJI Phantom 3 Standard has 4 cells all connected in series, with nominal voltage of 3.8 V per cell and nominal capacity of 4.480 Ah. The DJI Phantom is shown in figure 1.2 and the cell is shown in figure 1.3.

CHAPTER 2. BATTERY MODELING

This chapter will provide an in-depth analysis of common electronic elements and how to create a circuit that has similar behaviorial properties as the observed cell. Such circuit is referred to as an equivalent circuit model (ECM). ECMs give insight on how cells function under different loads and dynamic changes. When choosing an ECM to represent the observed cell, it is very important to balance between the circuit complexity, that will lead to unnecessary computational complications, and the modeling accuracy. ECMs have been extensively studied and applied to develop a battery management system. Additionally, Lithium polymer batteries have been widely modelled using ECMs [12]. Once the ECM of one DJI Phantom 3 standard cell is designed, the complete battery can be modeled by placing 4 cells in series. It is important to note that it has been assumed that all 4 cells are identical to simplify the process.

2.1 Circuit Topology

It is essential to make sure that the circuit topology chosen closely matches with the characteristics and the dynamics of the cell observed. The cells of the DJI Phantom 3 Standard are Lithium-Polymer with limited knowledge of internal chemistry.

2.1.1 State of charge dependence

Typically, the voltage of a fully charged Lithium-Polymer cell is higher than that of a discharged cell. This can be captured by relating the open-circuit voltage (OCV) to the state of charge (SOC) [12]. For the DJI Phantom 3 Standard cell, it is defined to be at 100% SOC when it is at 4.25 V and 0% SOC at 3.0 V. This will help in determining the OCV-SOC relationship needed in parameter estimation algorithm.

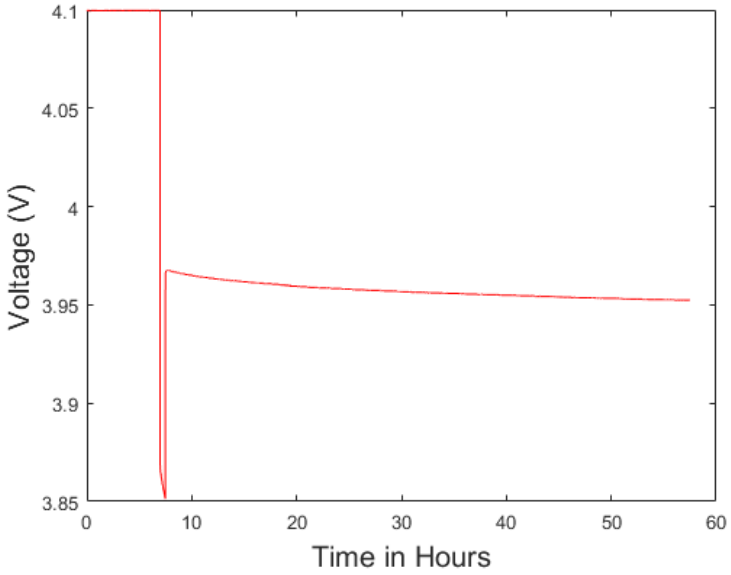

Figure 2.1: Example of a single pulse discharge

2.1.2 Resistance in series

Whenever a certain load is applied, the the cell's terminal voltage should drop below the open circuit voltage. In order to capture that phenomena, a resistor is placed in series with the voltage source. In general, the resistance would be dependent on the current and state of charge. For the purpose of this work, it will be assumed constant.

2.1.3 R-C circuits

When representing Lithium-Polymer cells in an ECM, Resistor-Capacitor circuits are an essential component. This is due to the fact that the number of R-C pairs determines the ability of the ECM to match with the measured responses from the cell testing [12]. To determine the number of R-C pairs that will be sufficient to well represent the observed cell, a single pulse discharge test followed by a relaxation period is performed and analyzed [12]. The relaxation period is then fitted into exponential equations of orders 1 and 2 that represent 1 R-C pair and 2 R-C pairs respectively. The fitting was done using MATLAB's Curve Fitting Toolbox.

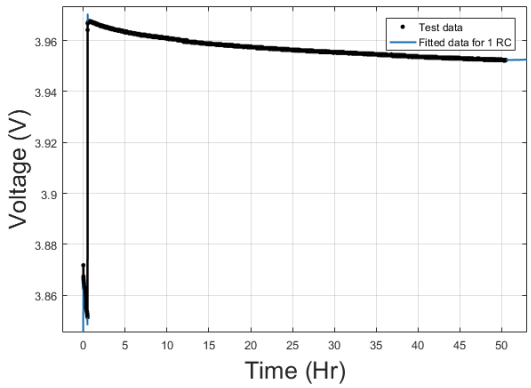

Figure 2.2: Fitted data for 1 RC

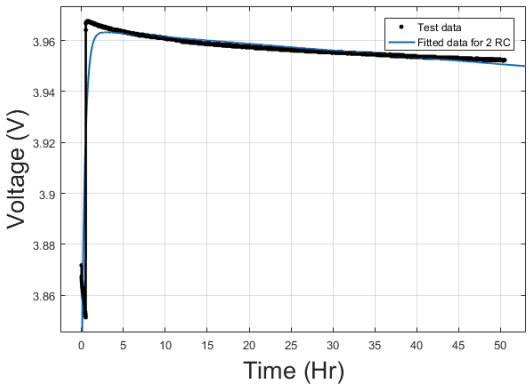

Figure 2.3: Fitted Data for 2 RC

Table 2.1: Comparison between the two fits

R-C Pairs	SSE	R^2	RMSE
1	0.0533	0.03273	0.001038
2	0.1666	0.7534	0.005243

Figures 2.2 and 2.3 show the results of the fitting algorithm for 1 R-C and 2 R-C pairs respectively. Table 2.1 show the comparisons between the two fitted curves. The 1 R-C pair has a lower sum of squared error and root mean squared error. This finding proves that 1 R-C pair provides a better representation of the observed cell than 2. 3 R-C and 4 R-C pairs were not investigated due to the fact that it adds a higher degree of complexity when it comes to the parameter estimation of the ECM and does not produce significant improvement in modeling accuracy.

2.1.4 Hysteresis voltage

So far, the ECM has a resistor, an open-circuit voltage, and a R-C pair all connected in series. With this circuit, if the current drops to zero, the voltage across the resistor in series drops to zero, and the voltage of the capacitor will exponentially drop to zero over time. This is not representative

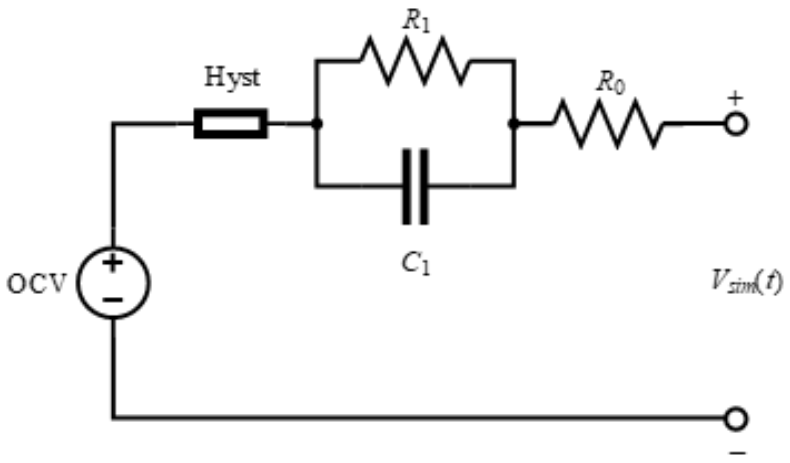

Figure 2.4: Final equivalent circuit model

of the observed cell, as its voltage may drop to a value considerably different than the open-circuit voltage, and this voltage drop is dependent on the cell's operation history. This phenomena is known as hysteresis [12].

The final ECM of the observed cell is shown in figure 2.4. As described in previous sections, the open circuit voltage is a function of SOC, and a single R-C pair is connected in series with a resistor and a hysteresis voltage. The final equation of the ECM is given by equation 2.1.

$$V_{out} = OCV(SOC) - i_0 R_0(SOC, i) - i_1 R_1(SOC, i) - MHyst \tag{2.1}$$

2.2 Cell Testing

Now that the topology of the ECM has been decided, it is important to conduct different types of tests on the observed cell to be able to estimate its parameters. These parameters are estimated by using the data from the tests, and fitting them into the model of equations that are representative of the ECM.

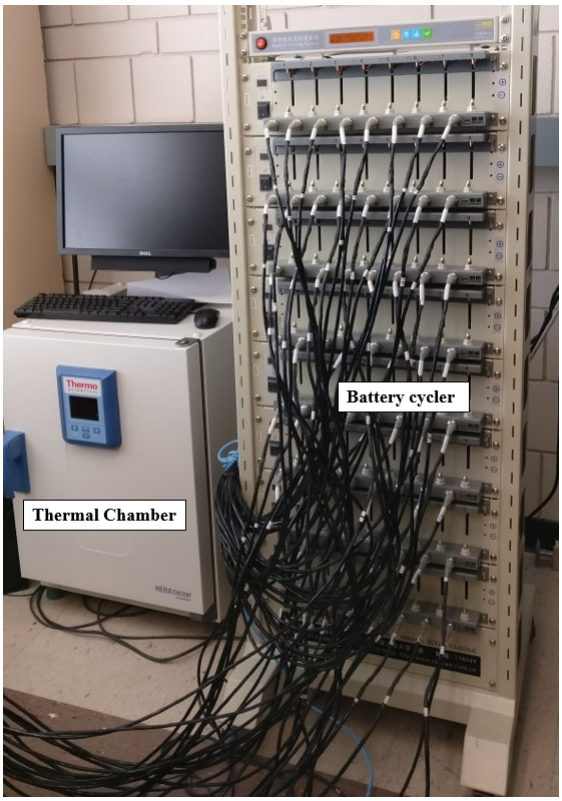

Figure 2.5: Battery testing system

The battery testing is performed at Iowa State University, in the System Reliability and Safety Laboratory located at the Mechanical Engineering department. The Battery Testing System is of model Neware BTS5V6A, with a power of 448 W, a voltage measurement range of 10 mV — 5V, and 12 mA — 6 A for both charging and discharging. This system can control a cell's current according to a user-fitted profile of applied current versus time, and in return records the cell's current and voltage. The test must be conducted in a temperature-controlled environment. The system can simultaneously perform tests on 8 different cells.

2.2.1 Static testing

A static test is conducted to determined the open-circuit voltage (OCV) as a function of state-of-charge (SOC). Before beginning the test, it is essential to ensure that the observed cell is fully charged, and if not, that is fully accounted for in the test script.

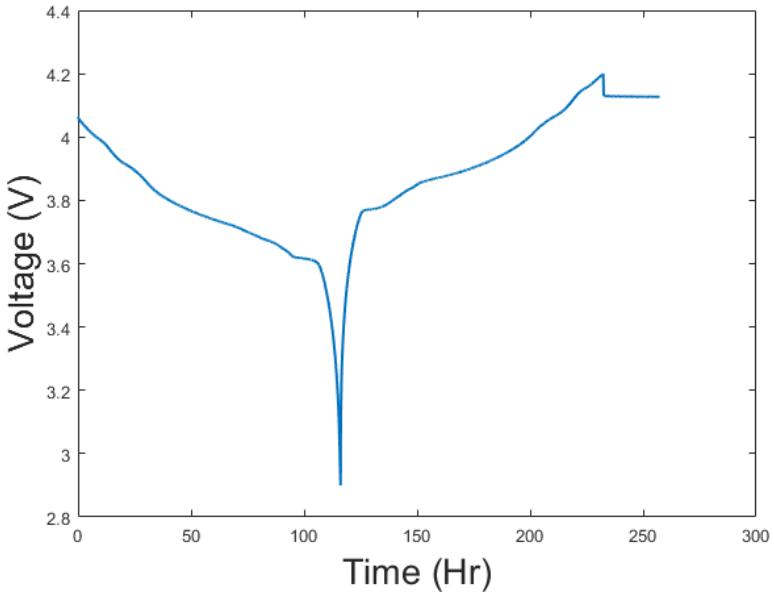

Figure 2.6: Example of a static cell test

2.2.1.1 Static testing script

1. Fully charge the cell to 100% state-of-charge and place it in a temperature-controlled chamber 2 hours before the test to ensure the temperature is uniform.

2. Discharge the cell at a constant current rate of $\frac{C}{30}$ until the voltage across the cell reaches its lower cut-off voltage of 3.0 V.

3. Charge the cell at constant current rate of $\frac{C}{30}$ until the voltage across the cell reaches its upper cut-off voltage of 4.25 V.

4. Use the voltage data from slow-dicharge/charge test to determine the open-circuit voltage of the cell.

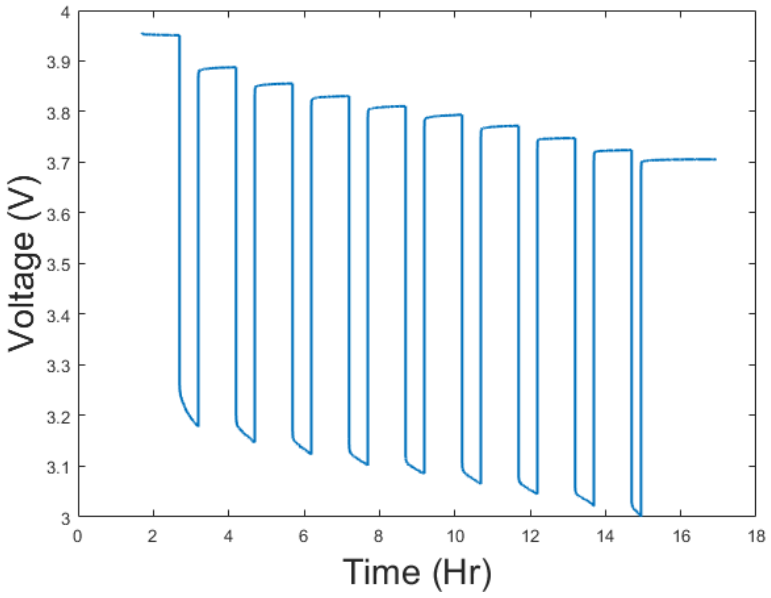

Figure 2.7: Example of a dynamic cell test

2.2.2 Dynamic testing

A dynamic test is conducted to determine the remaining equivalent circuit parameters. Before beginning the test, it is essential to ensure that the observed cell is fully charged, and if not, that it is fully accounted for in the test script. An example of such test is shown in figure 2.7.

2.2.2.1 Dynamic testing script

1. Fully charge the cell to 100% SOC and place it in a temperature-controlled chamber 2 hours before the test to ensure the temperature is uniform.

2. Discharge the cell at a constant current rate of $\frac{C}{50}$ (different c-rates are used) until the the cell loses 10% of its capacity.

3. Allow the cell to relax for a specified period of time.

4. Carry out dynamic profiles over SOC range of 90% to 10%.

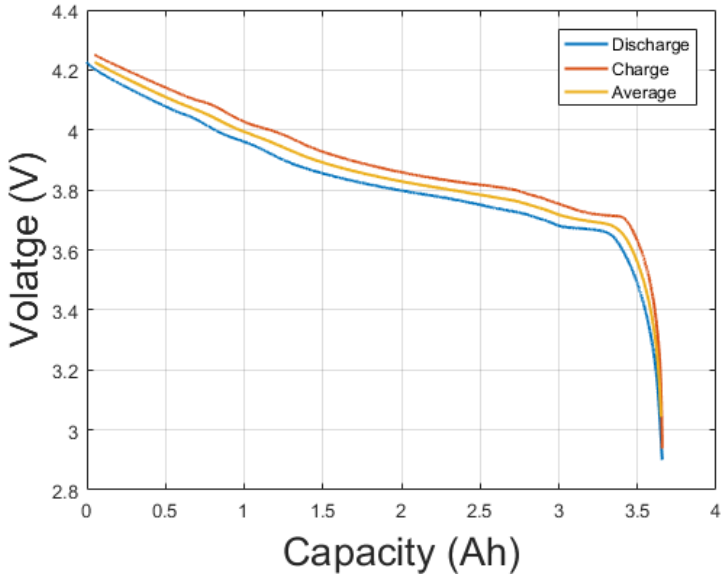

Figure 2.8: Voltage vs. Capacity for charging, discharging, and average

5. Charge the cell at a constant current rate of $\frac{C}{50}$ until voltage across the cell reaches its maximum.

2.3 Circuit Parameter Estimation

2.3.1 Open circuit voltage/state-of-charge relationship

From conducting a full charging/discharging static test on the cell observed, the open-circuit voltage/state-of-charge relationship is determined as follows:

- Observe how the voltage changes with respect to capacity for the charging and discharging cycles respectively.
- Compute an average between both observations as shown in figure 2.8.
- Use the final averaged voltage-capacity result to compute the depth of charge at each time step t:

$$DOC(t) = \frac{Q(t)}{Q_{Total}} \tag{2.2}$$

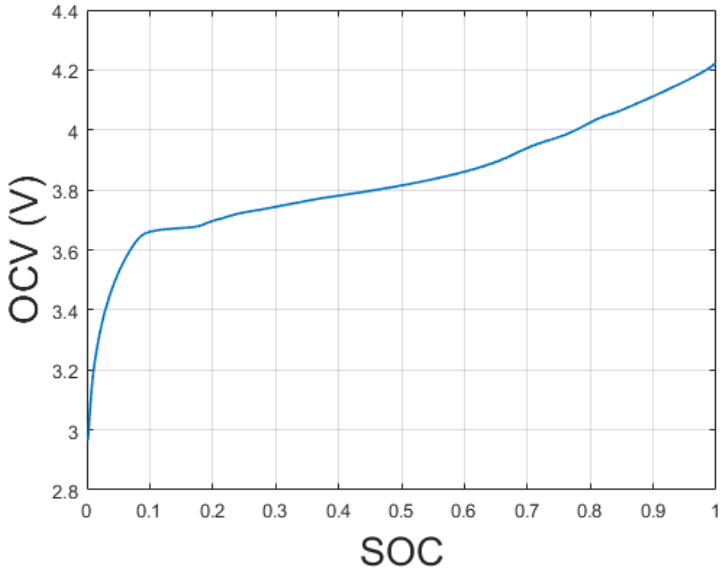

Figure 2.9: Final OCV vs SOC relationship

- SOC at each time step is then computed by:

$$SOC(t) = 1 - DOC(t) \tag{2.3}$$

- The final OCV and SOC plot is shown in figure 2.9

2.3.2 Remaining ECM parameters

The objective of the parameter estimation algorithm is to obtain a set of parameters that can be used in model to best predict a certain behavior. In this case, the parameters will be used in the ECM to predict voltage response of a cell with a given stimuli; the controlled current input. The accuracy of the prediction will be the criteria for determining the parameters. The root mean square error (RMSE) between predicted and measured voltage will be used to determined the accuracy of the prediction. Since no analytical solution of the best parameter values can be acquired, stochastic algorithm is applied to get the best estimates of those parameter values. Particle Swarm Optimization (PSO) is used for the purpose of this estimation. The algorithm will start with reasonable guesses of those parameters since boundaries can be set for the parameter

values given prior knowledge of the cell exists. The algorithm will then search in the parameter space and try to minimize the defined cost function. When a minimum of the cost function is reached, the algorithm will stop and give you a set of 'best-fit' parameters.

2.3.2.1 Particle Swarm Optimization

Algorithm 1 Particle Swarm Optimization

```
Start with a population of particles and choose a random value for positions and velocities in search space
while Termination condition not reached do
    for Each particle i do
        Calculate the velocity of the particle
        Update the position of the particle
        Evaluate the fitness of Particle f(X⃗_i)
        if f(X⃗_i) < f(P⃗_i) then
            P⃗_i ← X⃗_i
        end if
        if f(X⃗_i) < f(P⃗_g) then
            P⃗_g ← X⃗_i
        end if
    end for
end while
```

PSO is a stochastic optimization algorithm that uses population based approach to find the global minimum. Algorithm 1 shows the details of how the PSO algorithm works [13]. $f(\overrightarrow{P}_i)$ is best fitness value for particle i. P_g is the particle with the best fitness value of all particles. The algorithm will terminate when the function tolerance is less than or equal to 1×10^{-6}. The population size for this problem was set to 60. The measure of fitness of this problem is the objective function defined in 2.4.

2.3.2.2 Optimization Problem Formulation

PSO requires a definition of the variables, objective function, and constraints of the parameter estimation problem.

Variables

1. x_1 : the resistance of the resistor in series R_0.
2. x_2 : the time constant of the RC circuit τ.
3. x_3 : the resistance of the RC circuit resistor R_1.
4. x_4 : the hysteresis factor *itea*.
5. x_5 : the factor multiplied by the hysteresis voltage M.
6. x_6 : the constant multiplied by the sign of the current M_0

Optimization Model

$$\begin{aligned} \min \quad & \sqrt{\frac{\sum_{t=1}^{n}(V_m - V_s(x_1, x_2, x_3, x_4, x_5, x_6))^2}{n}} \\ \text{s.t.} \quad & 0.00 \leq x_1 \leq 1.00 \\ & 10.00 \leq x_2 \leq 2000 \\ & 0.00 \leq x_3 \leq 2.00 \\ & -1.00 \leq x_4 \leq 1.00 \\ & -\infty \leq x_5 \leq +\infty \\ & -0.01 \leq x_6 \leq 0.01 \end{aligned} \tag{2.4}$$

where V_m is the measured voltage from the dyanmic testing, n is the length of V_m vector, and V_s is simulated voltage given by equation 2.1.

Table 2.2: Estimation results

Test	R_0	τ	R_1	Itea	M	M_0
1	0.00756	111.114	0.0389	-0.0084	12.1153	0.0100
2	0.00965	150.457	0.0487	-0.0091	26.4412	0.0100
3	0.00458	110.983	0.0583	-0.0088	29.3275	0.0100
4	0.00634	108.631	0.0377	-0.0056	12.3261	-0.0100

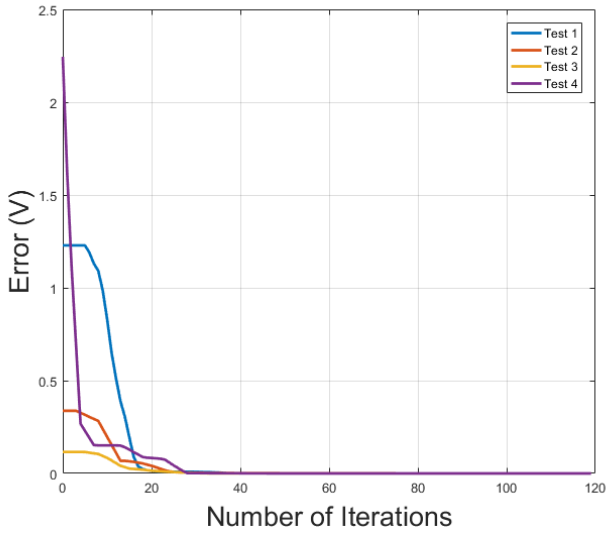

Figure 2.10: Optimality convergence for all tests

2.3.2.3 Results

Four different types of dynamic tests were conducted on the observed cell to be used in parameter estimation algorithm:

1. 1.3 C pulse discharge followed by a 1 hour relaxation period.

2. 1 C pulse discharge followed by 1 hour relaxation period.

3. 0.5 C pulse discharge followed by a 1 hour relaxation period.

4. 0.3 C pulse discharge followed by a 1 hour relaxation period.

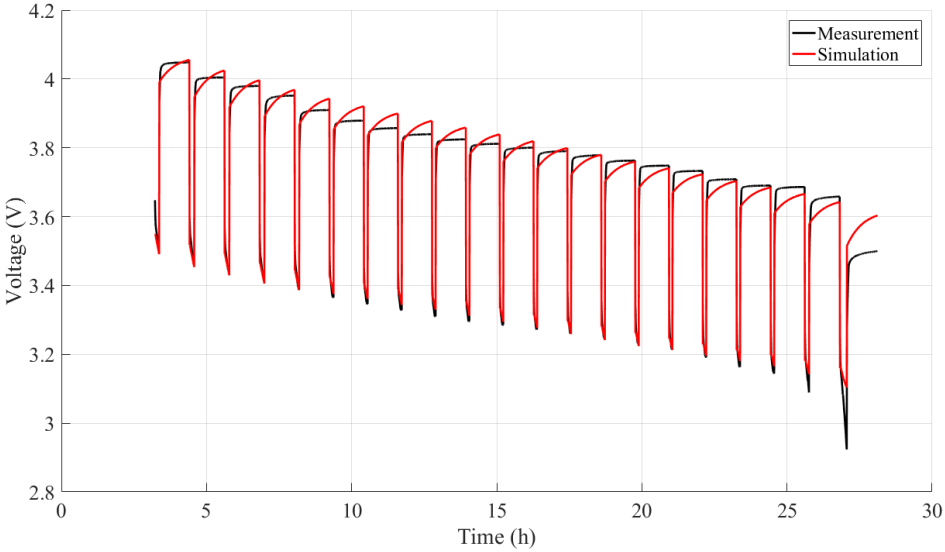

Figure 2.11: 1.3 C, 1 hour relaxation

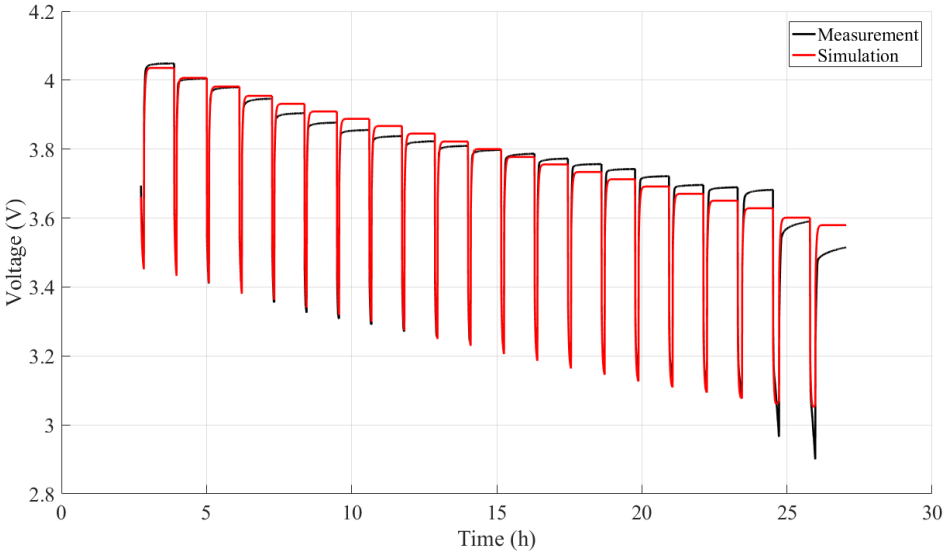

Figure 2.12: 1 C, 2 hour relaxation

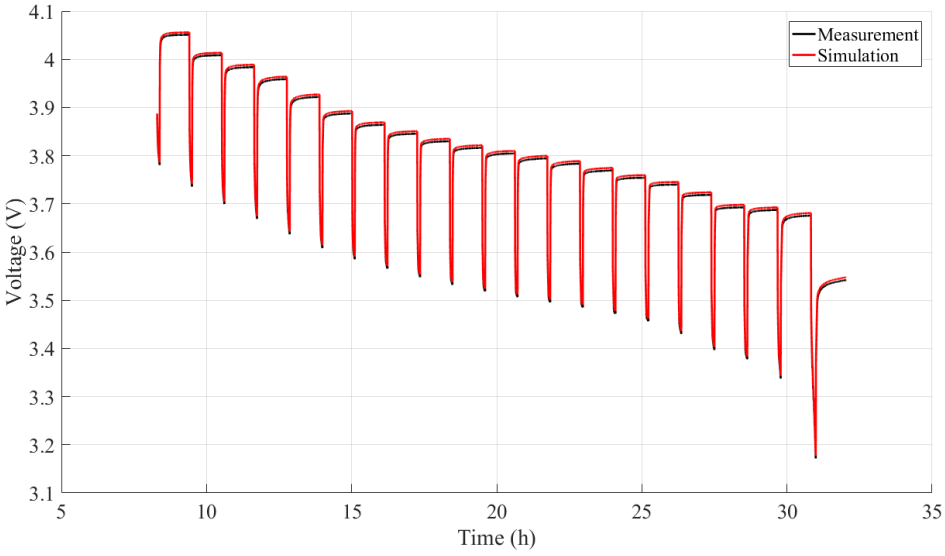

Figure 2.13: 0.5 C, 1 hour relaxation

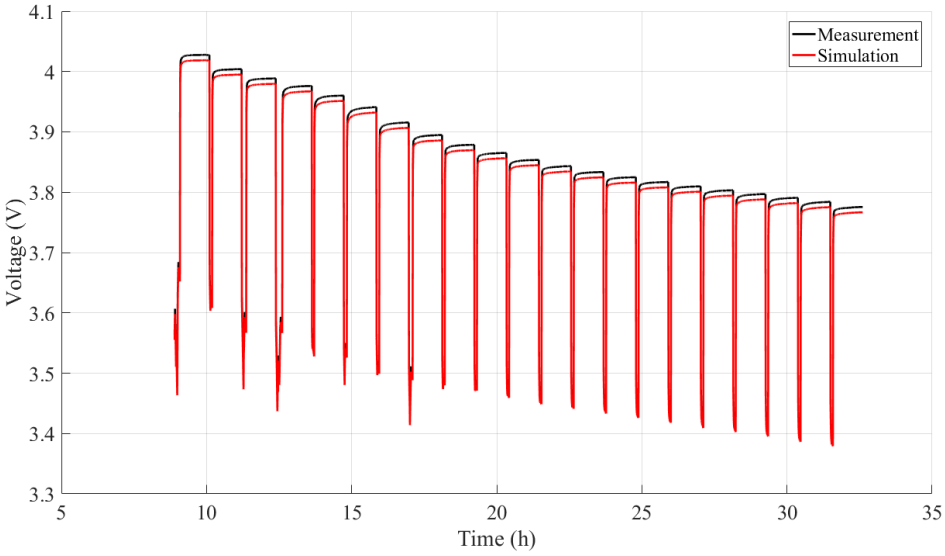

Figure 2.14: 0.3 C, 1 hour relaxation

The results of the parameter estimation of each of the four tests are shown in table 2.2. The optimization algorithm for each of the four tests resulted in close estimations of the parameters, which concludes the accuracy of the approach and the parameters. If the cell's performance is stable, then the parameter optimization results should be similar for different tests. In this case, the parameters from each of the tests are close, so averages are taken in order to determine the final equivalent circuit model parameters.

Figure 2.10 shows the error in Volts between the global minimum of $f(x)$ and the minimum found at each iteration for all the four tests. The results from figures 2.11, 2.12, 2.13, and 2.14 clearly show how accurate the parameter estimation algorithm is as the simulated voltage response matches closely with the measured voltage from the testing.

CHAPTER 3. POWER DEMAND MODELING

This chapter will describe how the power demand profile for a specific flight plan can be predicted from the specific flight plan and prior knowledge of the dynamics of the quadrotor.

3.1 Performance data

The DJI Phantom 3 Standard has a set of performance data that are important for the implementation of this algorithm shown in table 3.1.

3.2 Dynamics Model

For the purpose of this study, only forward flight will be considered. This means that there will be no ascend/dcesend phases incorporated in the analysis of the power demand. Using the dynamic model in [14]:

$$T\sin\theta - Dcos\gamma = 0 \tag{3.1}$$

$$\frac{dV_h}{dt} = \frac{T\cos\theta - D\sin\gamma - mg}{m} \tag{3.2}$$

where α is the angle of attack, θ is the pitch angle of the vehicle, and γ is the flight path angle.

3.2.1 Momentum theory for forward flight

Since this work will only examine forward flight, it is critical to capture the dynamics of such flight accurately. For a quadrotor, the induced velocity v_i is [15]:

$$v_i = \frac{v_h^2}{\sqrt{(v_\infty cos\alpha)^2 + (v_\infty sin\alpha + v_i)^2}} \tag{3.3}$$

Table 3.1: Performance Data of DJI Phantom

Performance Data	Value
Weight (Battery & Propellers Included)	1380 g
Max horizontal speed	16 m/s
Rotor disk area	0.0452 m^2
Vehicle Frontal Area	$139 \times 10^{-4} m^2$

where v_h is the induced velocity at hovering, α is the angle of attack, and v_∞ is the steam velocity. Since v_i is on both ends of the equation, computational methods are needed to solve it [15].

$$P_{Total} = \frac{1}{\eta_P}\frac{1}{\eta_e}T_{Total}(v_\infty \sin\alpha + v_i) \tag{3.4}$$

$$\eta_P = 0.7652 \tag{3.5}$$

$$\eta_e = 0.85 \tag{3.6}$$

where η_P and η_e are the propeller and power conversion efficiencies respectively, which have been referenced from [8]. The main reason these inefficiencies are added to the model is to reinstate that the predicted power demand will always be lower than the actual power required by the UAS. Since the blades are of a finite number, as opposed to the assumption of infinite number of blades in momentum theory, the tip will always produce vortices, and that leads to a flow that is not a linear laminar flow, which is accounted by η_P. Additionally, the power produced by the motor will not be fully transformed into the rotor due to mechanical inefficiencies, and that is accounted by η_e. The underlying work to account for these inefficiencies have been discussed in details in Chapter Two of [16].

3.2.2 Drag model

Since only forward flight will be considered for this study, the drag model, shown in equation 3.7 is only one dimensional and is along the horizontal path. Only parasite drag will be considered

for the purpose of this work [14].

$$D = \frac{\rho v_\infty^2 C_D F A}{2} \tag{3.7}$$

where ρ is the density of air at the specified altitude, C_D is the drag coefficient of 1.0, and FA is the frontal area of the UAS.

CHAPTER 4. MISSION ASSESSMENT

This chapter will explain the flight testing conducted on the DJI Phantom 3 Standard, which will be an essential component in the state estimation algorithm. Additionally, this chapter will explain how the online prediction algorithm works.

4.1 Flight Testing

Upon starting the DJI GO application, a connection is established with the Phantom and data is recorded (current, voltage, GPS coordinates, and velocity in all three axis). This file is stored locally on the device, and can be accessed from device settings or by connecting to a computer.

The user may then input, using the interface of the application, the parameters for the flight. From here, a series of way points along the path is computed to match those parameters. These way points are then combined into a mission and uploaded to the Phantom 3 Standard before the flight is started. This was done using the DJI mobile SDK. The DJI mobile SDK appears to prevent multiple active connections across applications (i.e. the inability to use DJI GO and SDK at the same time). Instead, switches can be made between the two by exiting and terminating the other.

The flight test conducted on the DJI Phantom 3 Standard consisted of two way points as shown in figure 4.1, where the UAS continuously performs back and forth laps until the battery drains.

4.2 State Estimation

After conducting the flight testing and archiving the voltage and current profiles, they will be used to validate the accuracy of the equivalent-circuit model as shown in figure 4.2. The current profile from the flight testing is fed into the ECM, which will output an estimated voltage profile that will then be compared to the real voltage profile from the flight testing. Additionally, the state of charge profile will be estimated.

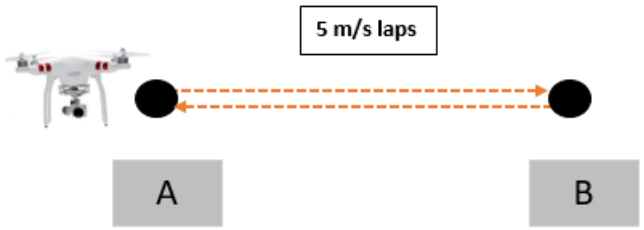

Figure 4.1: Flight plan

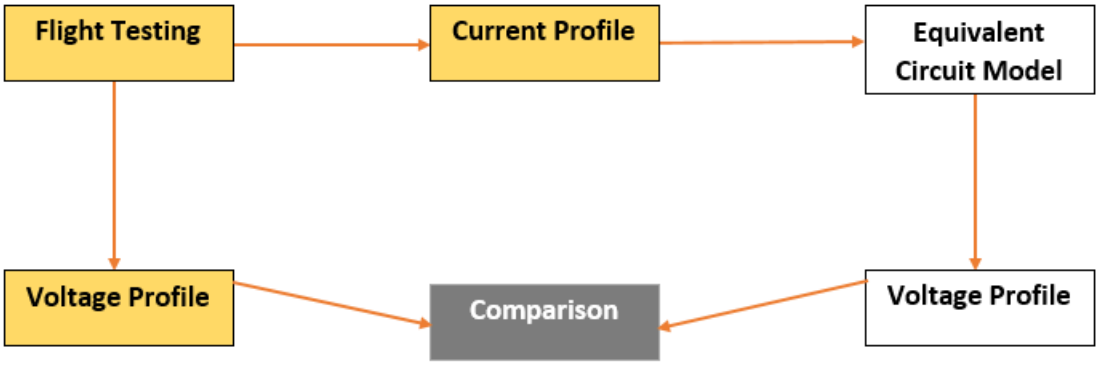

Figure 4.2: Estimation algorithm

4.2.1 Estimation Results

Figure 4.3 shows the current profile for the flight test conducted. From figure 4.4, the difference between the simulation and flight testing is about 0.05 V, which is quite accurate considering the assumptions that were reinstated in the ECM.

Figure 4.5 shows how the SOC changes with time using the estimation algorithm. It is important to note here that the estimation of the SOC doesn't reach zero, and that is representative in the fact that DJI Phantom 3 Standard has to terminate the mission and return to home when the battery charge is at 10%.

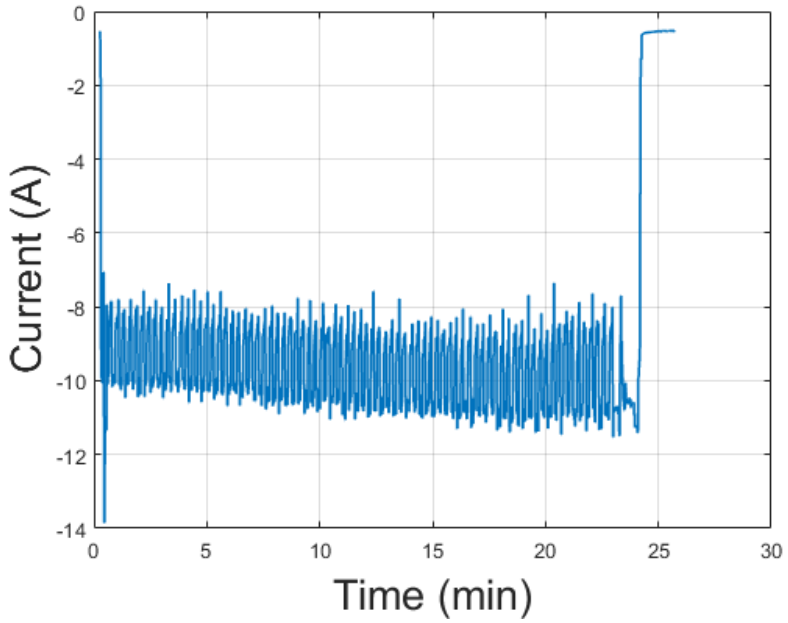

Figure 4.3: Current profile

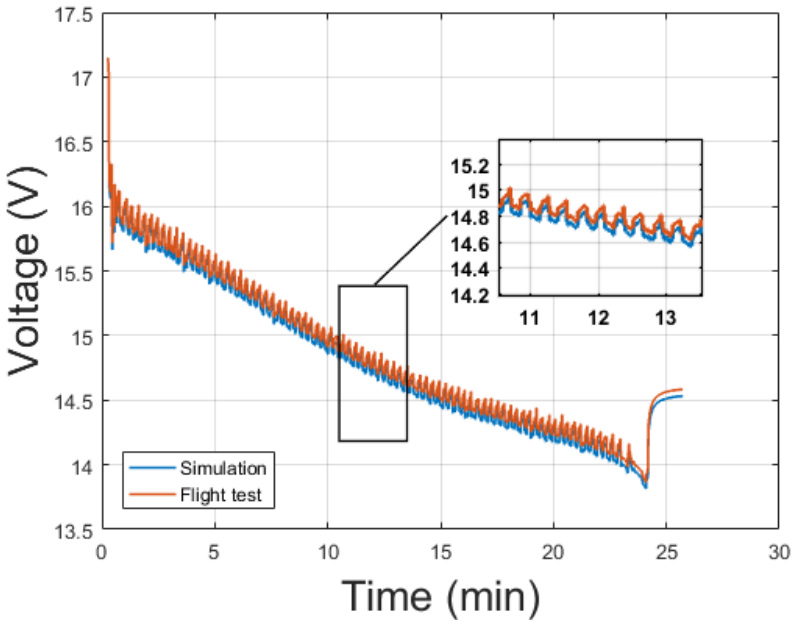

Figure 4.4: ECM-simulated voltage vs. measured voltage during flight test

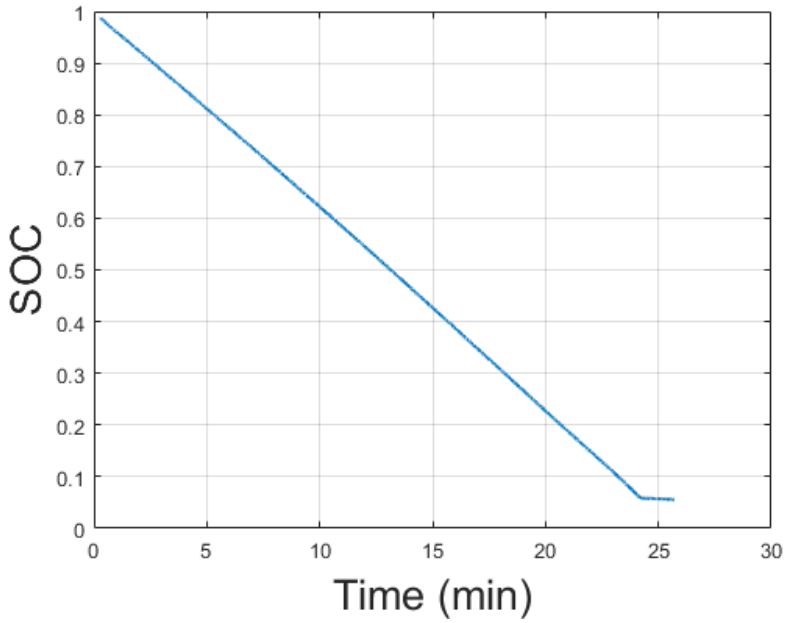

Figure 4.5: Estimated SOC vs. flight time

4.3 Online Prediction

Now that the equivalent circuit model has been validated with the flight testing, and the accuracy was within 0.05 V, it can be then used to predict the ability of a UAS to complete a specific flight plan. Figure 4.6 explains how the online prediction algorithm works. From a specific flight plan, and having prior knowledge of the dynamics of the UAS, the future power demand can be estimate as described in chapter 3, which can be then fed into the ECM to get voltage and SOC profiles. It is critically important to define a cut-off voltage, after which the battery no longer has any energy left. For the DJI Phantom 3 Standard, the cut-off voltage was assumed to be 12 V.

Figure 4.7 explains in details how the voltage can be estimated from the power demand profile. Assuming prior knowledge of the initial states ($V_{out,1}$, OCV_1, SOC_1, and i_1), the SOC at the second time step (SOC_2) can be estimated by:

$$SOC_2 = SOC_1 + \frac{i_1 \Delta t}{Q} \tag{4.1}$$

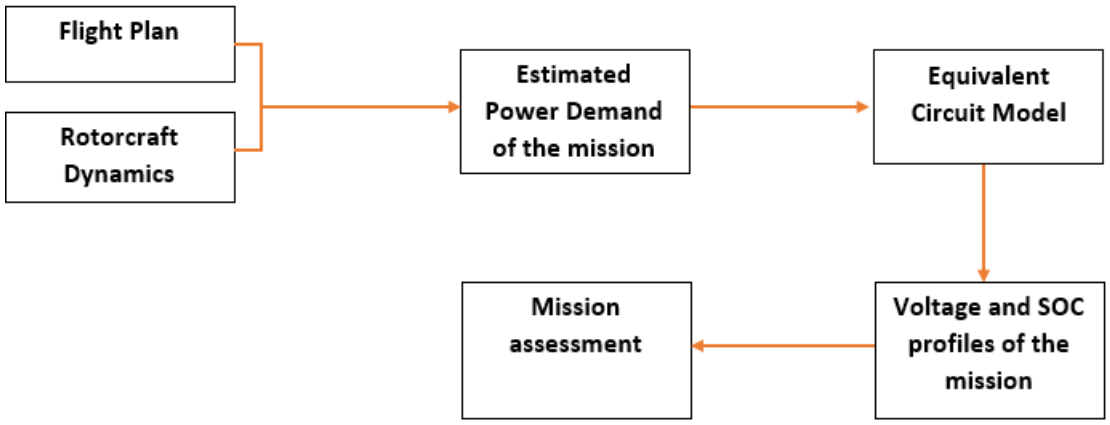

Figure 4.6: Prediction algorithm

where Δt is the time difference between the two steps, and Q is the total charge of the cell. The corresponding OCV_2 can be found from the SOC-OCV relationship determined in chapter 2. $V_{out,2}$ can be then determined from the ECM with equation 2.1. The current at the next step is then (i_2):

$$i_2 = \frac{P_2}{v_{out,2}} \tag{4.2}$$

This is an iterative process that will cover the whole power demand profile.

4.3.1 Case Study

A case study is created to help validate the the online prediction algorithm. The DJI starts from a hovering position, then accelerates to 10 m/s, moves forward at constant speed for a specified period of time, then decelerates back to zero as shown in figure 4.8. Using the equations and dynamics model defined in chapter 3, the power profile for the case study is shown in figure 4.9.

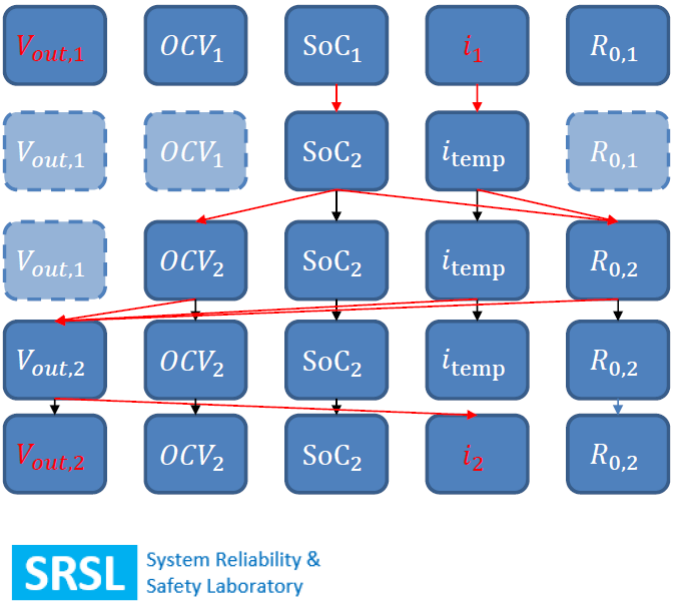

Figure 4.7: Voltage profile from power demand

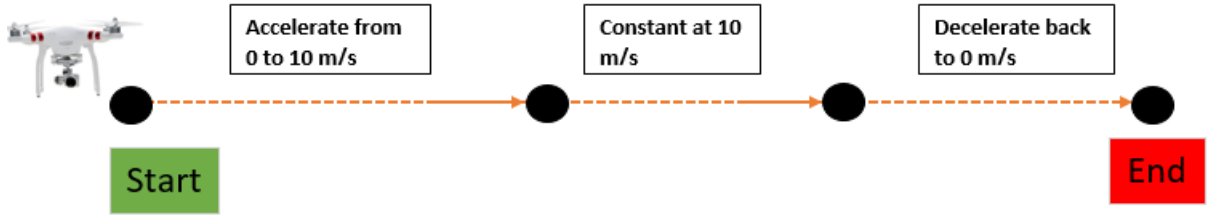

Figure 4.8: Case study

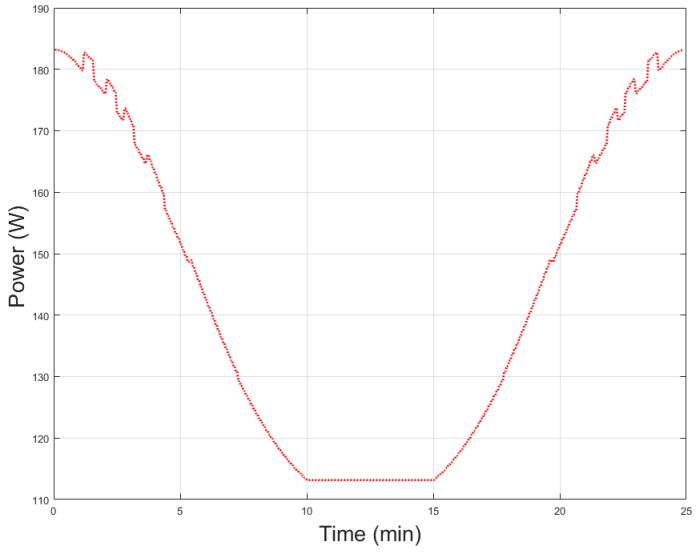

Figure 4.9: Estimated power demand

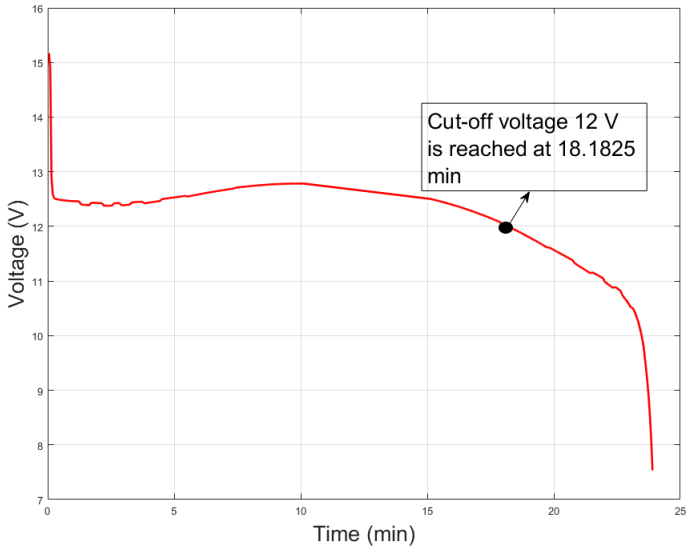

Figure 4.10: Voltage profile of case study

Using the equivalent circuit model, the voltage and SOC profiles are then predicted. Figures 4.11 and 4.10 show the results of that prediction.

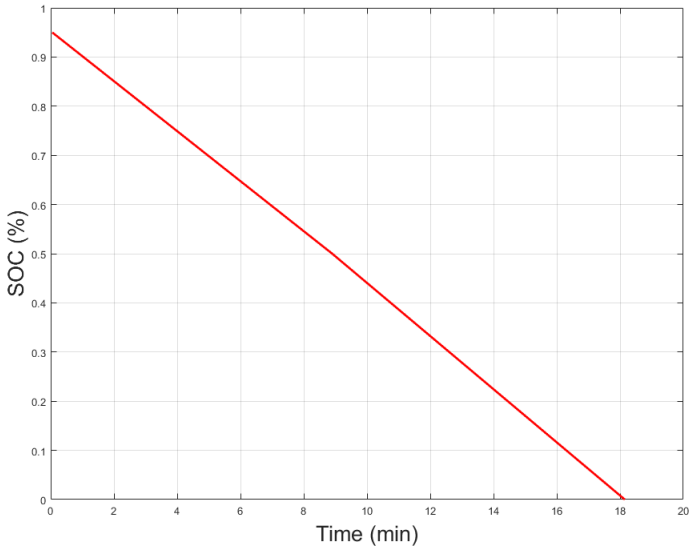

Figure 4.11: SOC profile of case study

As can be deduced from figure 4.10, the cut-off voltage of 12 V was reached at around 18.1825 minutes, which means that the DJI does not have enough power to complete this specific flight plan. Even though this case study has not been validated, it has a logical basis to it as the average time of the DJI Phantom 3 Standard is around 18 – 25 minutes. Additionally, the SOC profile confirms that the mission ends at 18.1825, because at that time instant the predicted SOC is 0%.

CHAPTER 5. CONCLUSION AND FUTURE WORK

In conclusion, this work presents a framework to be able to assess a UAS's ability to complete a flight plan. This work outlines how to choose the topology of the ECM with the aid of curve fitting of some cell testing data. Additionally, this work shows how dynamic and static cell testing data is used to help estimate the parameters of the ECM with the aid of Particle Swarm Optimization. Once the ECM has been created and the parameters have been estimated, validation was necessary to ensure the accuracy of the model; flight testing was used for that purpose, as voltage and current profiles were archived. The voltage profile from the flight testing is then compared to that from the estimation algorithm proposed in this work. The accuracy between both was within a maximum difference of about 0.05 V. Furthermore, the online prediction algorithm discussed was accurate to a certain extent, where the cut-off voltage was reached at around 18.1 minutes, which is within the time range of the DJI Phantom 3 Standard.

There were a lot of assumptions made in this work that could result in the inaccuracies present thus far. Firstly, the analysis was only done on one cell, and all the other cells were assumed to be identical. This may not be an accurate representation as cells might behave differently in the UAS. Furthermore, there was no previous knowledge of the cell's chemistry, which could've been helpful in understanding how it acts under different dynamic loadings. The work here can be extended by predicting the Remaining Useful Time (RUT) as a function of the flight operation time for a specific UAS. This relationship better represents the ability of a UAS to successfully finish a mission. This work can be significant in low altitude airspace operations, as it can assess a UAS's ability to successfully complete a mission by constantly predicting the battery behavior.

BIBLIOGRAPHY

[1] FAA, "FAA Releases 2016 to 2036 Aerospace Forecast," 2016, [Online; accessed 16-November-2017].

[2] Kopardekar, P. H., "Unmanned aerial system (UAS) traffic management (UTM): Enabling low-altitude airspace and UAS operations," 2014.

[3] "Revising the Airspace Model for the Safe Integration of Small Unmanned Aircraft Systems," 2015, [Online; accessed 16-November-2017].

[4] "Google UAS Airspace System Overview," 2015, [Online; accessed 16-November-2017].

[5] Mueller, E., "Enabling Airspace Integration for High-Density On-Demand Mobility Operations," .

[6] Holmes, B. J., Parker, R. A., Stanley, D., and McHugh, P., "NASA Strategic Framework for On-Demand Air Mobility," Tech. rep., NASA Headquarters, 01 2017.

[7] "Fast-Forwarding to a Future of On-Demand Urban Air Transportation," Tech. rep., Uber, 10 2016.

[8] Bole, B., Daigle, M., and Gorospe, G., "Online prediction of battery discharge and estimation of parasitic loads for an electric aircraft," *ESC*, Vol. 2, 2014, pp. 5S2P.

[9] Bole, B., Teubert, C. A., Cuong Chi, Q., Hogge, E., Vazquez, S., Goebel, K., and George, V., "SILHIL Replication of Electric Aircraft Powertrain Dynamics and Inner-Loop Control for V&V of System Health Management Routines," 2013.

[10] "Commercial Drone popularity by N number," 2016, [Online; accessed 17-November-2017].

[11] "Smart Battery," 2017, [Online; accessed 17-November-2017].

[12] Plett, G. L., *Battery Modeling*, 2015.

[13] Kennedy, J. and Eberhart, R., "Particle swarm optimization," *Neural Networks, 1995. Proceedings., IEEE International Conference on*, Vol. 4, Nov 1995, pp. 1942–1948 vol.4.

[14] Priyank Pradeep, P. W., "Energy Efficient Arrival with RTA Constraint for Urban eVTOL Operations," 2017.

[15] Hoffmann, G. M., Huang, H., Waslander, S. L., and Tomlin, C. J., "Quadrotor helicopter flight dynamics and control: Theory and experiment," 2007.

[16] Johnson, W., *Helicopter theory*, Courier Corporation, 2012.